Low Temperature Physics/Fizika Nizkikh Temperatur, 2018, v. 44, No. 12, pp. 1630–1638

Nonlocal optical response of a layered high-temperature superconductor slab

S. Cortés-López and F. Pérez-Rodríguez

Instituto de Física, Benemérita Universidad Autónoma de Puebla
Apartado Postal J-48, Puebla, Pue. 72570, México
E-mail: scortesl@ifuap.buap.mx

Received July 4, 2018, published online October 26, 2018

We theoretically study the effect of the spatial dispersion on the optical response of a layered high-temperature superconductor slab. The nonlocality of the inherently-anisotropic layered superconductor comes from the wave vector dependence of its average permittivity tensor, and leads to the generation of additional electromagnetic modes just above the characteristic Josephson plasma frequency, that is in the terahertz range. We calculate p-polarization optical spectra for a $Bi_2Sr_2CaCu_2O_{8+\delta}$ (Bi2212) superconductor slab, which show very narrow resonances associated with the quantization of the wave vectors of both long-wavelength electromagnetic modes, having negative dispersion, and short-wavelength additional (nonlocal) modes of positive dispersion. The dependence of the frequency position and shape of the resonances on the nonlocality parameter, the slab thickness, and the components of the quasiparticle conductivity is analyzed. We have found that the quantized long-wavelength modes of negative dispersion, which can only be observed at relatively-large slab thicknesses, give rise to prominent resonances in the p-polarization reflectivity spectrum. On the other hand, the resonances associated with quantized additional short-wavelength electromagnetic modes are weak, but they can be clearly observed when the superconductor slab thickness is smaller than the smallest magnetic-field penetration depth.

Keywords: layered superconductors, cuprate superconductors, metamaterials, spatial dispersion, thin films.

1. Introduction

The electrodynamic properties of layered high-temperature superconductors is of great interest because of their applications in the THz frequency range [1–3] and are well described by using the model of a periodic system with intrinsic Josephson junctions in the unit cell [4–9]. As was demonstrated in several works (see, for example, the reviews [8,9] and references therein), the gauge-invariant phase difference of the order parameter in the junctions obeys sine-Gordon equations, whereas the electric and magnetic fields in the laminar superconductor are determined from the distribution of such a phase difference. Among the striking phenomena described by sine-Gordon equations, the stop-light effect and the excitation of Josephson plasma waves (JPW) have been of particular interest [8].

The JPW can be excited by a p-polarized electromagnetic wave incident on the high-temperature superconductor surface, parallel to the *ab* plane. In the case of small wave amplitudes (linear regime), the dispersion relation between the wave vector component $k_z^{(s)}$, parallel to the c axis, and the frequency ω for propagating modes in a layered superconductor like Bi2212 has two branches at frequencies above the characteristic Josephson plasma frequency, being in the terahertz (THz) range [8,10]:

$$\omega_p = c/(\lambda_\perp \sqrt{\varepsilon}). \tag{1}$$

Here, $\lambda_\perp$ is the transverse magnetic field penetration depth, ε is the high-frequency dielectric constant of the insulating layers alternating with superconducting layers, and c is the light velocity in vacuum. It turns out that one of the branches has negative dispersion ($\partial\omega/\partial k_z^{(s)} < 0$), whereas the dispersion of the second one is positive ($\partial\omega/\partial k_z^{(s)} > 0$). The appearance of the later branch is owing to the effect of the dynamical breaking of charge neutrality in the layered superconductor, which is controlled by the capacitive coupling parameter [8],

$$\alpha = \frac{\varepsilon R_D^2}{sD}, \tag{2}$$

where R_D is the Debye length for a charge in a superconductor, s is the thickness of a superconducting layer, and D is the period of the insulator-superconducting superlattice.

In the long-wavelength regime ($|k_z^{(s)}|D \ll 1$), the electromagnetic response of an inherently anisotropic layered

high-temperature superconductor can be described with an average nonlocal permittivity tensor $\overleftrightarrow{\varepsilon}_{av}$, whose components depend not only on the frequency ω, but also on the wave vector $k_z^{(s)}$ (see Refs. 10, 11). In the limit of charge neutrality, when the parameter $\alpha = 0$, the nonlocality of the layered superconductor and, consequently, the second (additional) branch of the dispersion relation $k_z^{(s)}(\omega)$ disappears. In the later case, the layered superconductor behaves as a hyperbolic metamaterial with effective negative refraction index. Indeed, as is shown in Ref. 11, at frequencies ω above the Josephson plasma frequency ω_p, the permittivity components, parallel and perpendicular to the superconducting planes, have different sign. Interesting electromagnetic phenomena in layered high-temperature superconductors have been described within the local approach. Thus, for example, the dispersion curves and the excitation of wave-guide [12–14] and surface Josephson plasma [12,14] waves in a superconductor slab, placed between two identical dielectrics, have been analyzed by using a local average permittivity tensor. Moreover, the local approach has been successfully applied in studying the resonant optic transmission through different heterostructures, containing a layered high-temperature superconductor slab, on which localized modes can be excited [15,16]. The local continuum limit has also allowed to describe the transmission of terahertz radiation through periodically modulated slabs of layered superconductor [17,18].

The Debye length in a superconductor is usually much smaller than the London penetration depth and, therefore, the nonlocality parameter α (2) is typically small. However, as is shown in Refs. 8, 10, 11, the breaking of the charge neutrality of the superconducting layers and the capacitive interlayer coupling can play an important role in the dispersion properties of the JPWs when the frequency ω is very close to the Josephson plasma frequency ω_p (1).

In the present work we shall study the nonlocal electromagnetic response of a layered high-temperature superconductor slab near the Josephson plasma frequency. A theoretical formalism, based on the use of an average nonlocal effective permittivity to calculate the electromagnetic field inside a superconductor slab, is described in Sec. 2. In the model, we apply additional boundary conditions, which allow us to determine the amplitudes of the additional electromagnetic modes. We calculate and analyze the dispersion relations for p-polarized modes and the optical (reflectivity) spectra for a Bi2212 superconductor slab in Secs. 3 and 4. Here, we also study the effect of the nonlocality parameter α upon the resonant structure of the optical spectra. Our conclusions are written in Sec. 5.

2. Formulation of the problem

2.1. Geometry of the system

The system considered here is a high-T_c superconductor slab of thickness "d", specifically Bi2212, whose structure is inherently layered and periodic. Its superconducting planes are assumed to be parallel to the $x-y$ plane and the system is embedded in vacuum (see Fig. 1). Also assuming that a monochromatic electromagnetic plane wave with p-polarization is incident on the superconductor-slab surface at $z = 0$, the magnetic field in the upper medium ($z \le 0$) can be written as

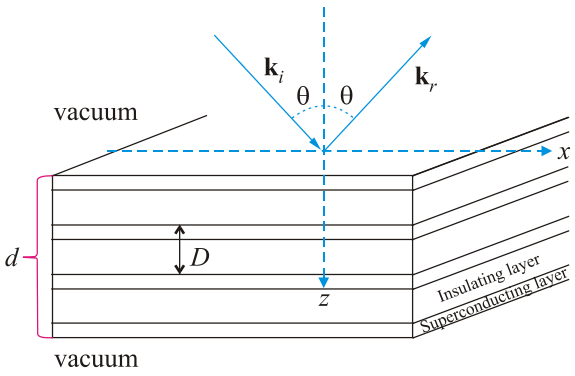

Fig, 1. Scheme of a high-temperature layered superconducting slab. $\mathbf{k}_i$ and $\mathbf{k}_r$ are the wave vectors of the incident and reflected light, respectively.

$$\mathbf{H}^{(u)} = \mathbf{H}_i + \mathbf{H}_r, \qquad z \le 0, \tag{3}$$

where the index "u" indicates the upper medium (vacuum), "i" the incident beam and "r" the reflected one. The expressions for $\mathbf{H}_i$ and $\mathbf{H}_r$ are, respectively,

$$\mathbf{H}_i = (0, H_i, 0)\mathrm{e}^{ik_x x + ik_z z - i\omega t}, \tag{4}$$

$$\mathbf{H}_r = (0, H_r, 0)\mathrm{e}^{ik_x x - ik_z z - i\omega t}, \qquad z \le 0. \tag{5}$$

In these expressions, $k_x = k\sin\theta$ and $k_z = k\cos\theta$ are the components of the incident wave vector $\mathbf{k}_i$, where $k = \omega/c$, ω is the frequency, and θ is the incidence angle. The magnetic field of the transmitted electromagnetic wave into the lower medium (vacuum) is given by

$$\mathbf{H}^{(t)} = (0, H_t, 0)\mathrm{e}^{ik_x x + ik_z (z-d) - i\omega t}, \qquad z \ge d. \tag{6}$$

2.2. Electromagnetic field in the superconductor slab

Now, to study the propagation of electromagnetic waves through a high-temperature layered superconductor, occupying the space $0 \le z \le d$, one can exploit the fact that the superconductor behaves as a uniaxial crystal in the long-wavelength limit [10,11]. As is shown in such works, the constitutive equation, relating the displacement vector $\mathbf{D}$ and the electric field $\mathbf{E}$,

$$\mathbf{D} = \overleftrightarrow{\varepsilon}_{av}\,\mathbf{E}, \tag{7}$$

is determined by a nonlocal average permittivity tensor $\overleftrightarrow{\varepsilon}_{av}$. The principal values of $\overleftrightarrow{\varepsilon}_{av}$ are functions of the wave number $k_z^{(s)}$ and frequency ω as

$$\varepsilon_x(\omega) = \varepsilon_y(\omega) = \varepsilon\left(1-\frac{\gamma^2\omega_p^2}{\omega^2}\right)+\frac{i4\pi\sigma_x}{\omega}, \tag{8}$$

$$\varepsilon_z(\omega,k_z^{(s)}) = \varepsilon\left[1-\frac{\omega_p^2\left(1+2\alpha(1-\cos(k_z^{(s)}D))\right)}{\tilde{\omega}^2}\right], \tag{9}$$

$$\tilde{\omega} = \frac{\omega}{\sqrt{1-i4\pi\sigma_z\dfrac{\omega}{\omega_p^2}\varepsilon}}, \tag{10}$$

where ω_p is the Josephson plasma frequency defined in Eq. (1), $\gamma = \lambda_\perp/\lambda_\parallel$ is the anisotropy parameter given by the ratio between the transverse ($\lambda_\perp$) and parallel ($\lambda_\parallel$) magnetic-field penetration depths, and D is the period of the array of insulating and superconducting layers. One should mention that expressions (8) and (9) were derived by assuming that the thickness of the superconducting layers s is much smaller than the lattice period D ($s \ll D$).

In the region of the superconductor slab, we will look for the solution for Maxwell equations as a p-polarized plane wave with a magnetic field given by

$$\mathbf{H} = (0, H_y, 0)e^{ik_z^{(s)}z+ik_x x-i\omega t}. \tag{11}$$

After substituting Eq. (7) and Eq. (11) into Faraday law ($c\nabla\times\mathbf{H} = \partial\mathbf{D}/\partial t$) and Ampere–Maxwell law for an anisotropic medium ($\mathbf{E} = (ic/\omega)\overleftrightarrow{\varepsilon}^{-1}\nabla\times\mathbf{H}$), we can derive the relations between the nonzero components of the electric and magnetic fields inside the superconductor:

$$\begin{aligned} ck_z^{(s)}H_y &= \omega\varepsilon_x(\omega)E_x,\\ ck_xH_y &= -\omega\varepsilon_z(\omega,k_z^{(s)})E_z,\\ k_xE_z - k_z^{(s)}E_x &= -(\omega/c)H_y. \end{aligned} \tag{12}$$

The dispersion relation for the electromagnetic waves inside the inherently-anisotropic layered superconductor can be straightforwardly obtained from the homogeneous system of algebraic equations (12). We get

$$\frac{(k_z^{(s)})^2}{\varepsilon_x(\omega)}+\frac{k_x^2}{\varepsilon_z(\omega,k_z^{(s)})} = \frac{\omega^2}{c^2}. \tag{13}$$

In order to obtain an explicit expression for the dispersion relation, we substitute Eq. (9) along with the next long-wavelength approximation ($|k_z^{(s)}|D \ll 1$),

$$(k_z^{(s)})^2 \approx \frac{2(1-\cos(k_z^{(s)}D))}{D^2} = \frac{4\sin^2((k_z^{(s)}D)/2)}{D^2}, \tag{14}$$

into Eq. (13). Afterwards, the dispersion relation for a p-polarized electromagnetic wave acquires the form

$$a\sin^4(k_z^{(s)}D/2)+b\sin^2(k_z^{(s)}D/2)+c = 0, \tag{15}$$

where

$$a = \frac{-16\alpha\omega_p^2\varepsilon D^2}{c^2},$$

$$b = 4\frac{\varepsilon}{c^2}(\tilde{\omega}^2-\omega_p^2)D^2+4\frac{\omega^2}{c^4}\varepsilon_x\varepsilon\alpha\omega_p^2D^4,$$

$$c = \frac{\tilde{\omega}^2}{c^2}k_x^2\varepsilon_xD^4-\frac{\omega^2}{c^4}\varepsilon_x\varepsilon(\tilde{\omega}^2-\omega_p^2)D^4.$$

By solving the biquadratic algebraic equation (15), we can explicitly express the wave number $k_z^{(s)}$ as a function of the frequency ω:

$$k_z^{(s)} = \pm\frac{2}{D}\arcsin\left(\sqrt{\frac{-b\pm\sqrt{b^2-4ac}}{2a}}\right). \tag{16}$$

Thus, four electromagnetic modes can propagate in the superconducting slab. The wave number of each mode will be denoted as follows:

$$k_z^{(j)}, \qquad j = 1, 2, 3, 4, \tag{17}$$

where $k_z^{(1)} = -k_z^{(3)}$ and $k_z^{(2)} = -k_z^{(4)}$ with the restrictions

$$\mathrm{Im}\,k_z^{(1)} > 0 \ \text{ and } \ \mathrm{Im}\,k_z^{(2)} > 0.$$

The latter implies that the first and second ($j = 1, 2$) electromagnetic modes decay along the positive direction of the z axis, whereas the third and fourth modes ($j = 3, 4$) decay in the opposite direction.

The total magnetic field inside the superconducting slab can be expressed as a linear superposition of the four electromagnetic modes:

$$\mathbf{H}^{(s)} = (0, H_y^{(s)}(z), 0)e^{ik_xx-i\omega t}, \tag{18}$$

where

$$H_y^{(s)}(z) = \sum_{j=1}^{4}A_je^{ik_z^{(j)}z}. \tag{19}$$

Here A_j ($j = 1, 2, 3, 4$) are the amplitudes of the plane waves.

From Eq. (19) and Faraday law, the x and z components of the electric field can be written in the form

$$E_x^{(s)}(z) = \frac{c}{\omega\varepsilon_x}\sum_{j=1}^{4}A_jk_z^{(j)}e^{ik_z^{(j)}z}, \tag{20}$$

$$E_z^{(s)}(z) = -\frac{ck_x}{\omega}\sum_{j=1}^{4}\frac{A_j}{\varepsilon_z(\omega,k_z^{(j)})}e^{ik_z^{(j)}z}. \tag{21}$$

2.3. Boundary conditions

In order to calculate the amplitudes A_j in Eq. (19), as well as the amplitudes of the reflected (H_r) and transmitted (H_t) electromagnetic waves, the well-known Maxwell boundary conditions should be applied, namely, the continuity of the tangential components of the electric and magnetic fields at the surfaces. These conditions for the vacuum-superconductor interfaces at $z = 0$ and $z = d$ are given by

$$E_x^{(u)}(0) = E_x^{(s)}(0), \qquad E_x^{(s)}(d) = E_x^{(t)}(d),$$
$$H_y^{(u)}(0) = H_y^{(s)}(0), \qquad H_y^{(s)}(d) = H_y^{(t)}(d). \qquad (22)$$

However, the number of unknown amplitudes is six (A_j, $j = 1, 2, 3, 4$; H_r and H_t) and the Maxwell boundary equations (22) are only four. Therefore, it is necessary to derive two additional boundary conditions (ABC) to calculate all the amplitudes. As in Ref. 10, we will derive the ABCs by taking into account the fact that the surface Josephson junctions have only one neighboring junction. In other words, there are no superconducting planes outside the slab. It means that the average of the polarization component, parallel to the growth direction of the layered superconductor, over the width of imaginary Josephson junctions just outside the slab should be equal to the polarization of the external medium.

For the anisotropic layered superconductor having a nonlocal dielectric response, the polarization vector can be written as

$$\mathbf{P}^{(s)} = (P_x^{(s)}(z), 0, P_z^{(s)}(z))\mathrm{e}^{ik_x x - i\omega t}. \qquad (23)$$

Here

$$P_x^{(s)}(z) = \chi_{e,x} E_x^{(s)}(z), \qquad (24)$$

where $\chi_{e,x} = (\varepsilon_x - 1)/4\pi$, $E_x^{(s)}(z)$ has the form (20) and

$$P_z^{(s)}(z) = \sum_{j=1}^{4} \chi_{e,z}(k_z^{(j)}) E_z^{(s)}(k_z^{(j)}) \mathrm{e}^{ik_z^{(j)} z}, \qquad (25)$$

with $\chi_{e,z}(k_z^{(j)}) = (\varepsilon_z(k_z^{(j)}) - 1)/4\pi$ and

$$E_z^{(s)}(k_z^{(j)}) = -\frac{ck_x}{\omega} \frac{A_j}{\varepsilon_z(\omega, k_z^{(j)})}. \qquad (26)$$

Since the external medium is vacuum, the polarization z-component, averaged over the width ($\approx D$) of imaginary Josephson junctions outside the sample, should vanish. Hence, the ABCs at $z = 0$ and $z = d$ can be written as

$$\frac{1}{D}\int_{-D}^{0} P_z^{(s)}(z)dz = 0, \qquad (27)$$

$$\frac{1}{D}\int_{d}^{(d+D)} P_z^{(s)}(z)dz = 0. \qquad (28)$$

Let us expand $P_z^{(s)}(z)$ into the Taylor series. We get

$$\frac{1}{D}\int_{-D}^{0} P_z^{(s)}(z)dz \approx \frac{1}{D}\int_{-D}^{0}\left(P_z^{(s)}(0) + \left.\frac{\partial P_z^{(s)}}{\partial z}\right|_{z=0} z\right)dz =$$
$$= P_z^{(s)}(0) - \frac{1}{2}D\left.\frac{\partial P_z^{(s)}}{\partial z}\right|_{z=0}, \qquad (29)$$

and

$$\frac{1}{D}\int_{d}^{d+D} P_z^{(s)}(z)dz \approx P_z^{(s)}(d) + \frac{1}{2}D\left.\frac{\partial P_z^{(s)}}{\partial z}\right|_{z=d}. \qquad (30)$$

In this way, the additional boundary conditions are

$$P_z^{(s)}(0) - \frac{1}{2}D\frac{\partial P_z^{(s)}}{\partial z}(0) = 0, \qquad (31)$$

$$P_z^{(s)}(d) + \frac{1}{2}D\frac{\partial P_z^{(s)}}{\partial z}(d) = 0. \qquad (32)$$

Applying these ABCs together with the Maxwell boundary conditions (22), the reflectivity ($R = |H_r/H_i|^2$) and transmissivity ($T = |H_t/H_i|^2$) spectra for the layered superconductor slab in the far infrared can be calculated.

3. Results

In this section, the theoretical formalism above presented is applied to study the propagation of p-polarization waves with $\theta = 75^\circ$ in a Bi2212 superconducting slab. The effects on the electromagnetic response of the superconducting slab due to the variation of the nonlocality parameter, the energy dissipation parameters, and slab thickness are all analyzed here. First, we have studied the effect of the nonlocality parameter on the dispersion relation for the electromagnetic propagating modes and far-infrared reflectivity spectrum. Three cases are described and discussed below.

3.1. Quasi-local case

The dispersion relation for the propagating modes when the nonlocality parameter α is almost zero is shown in Fig. 2(a), and the corresponding reflectivity is presented in Fig. 2(b). The superconductor parameters used in the calculations are [11]: $\omega_p = 10^{12}$ rad/s, $\gamma = 500$, $\varepsilon = 12.0$. Other parameters are $\alpha = 10^{-7}$, $d = \delta$, where δ is the smallest of the penetration depths for the anisotropic superconductor ($\delta = \lambda_{\|} = c/(\gamma\omega_p\sqrt{\varepsilon}) = 173.20$ nm), and $D = 15.35$ Å. In order to compare these results with our previous calculations for the local case ($\alpha = 0$) and without dissipation, published in Ref. 13, we have considered not just a very small value of α but also very small energy losses determined by the parallel and perpendicular conductivities of the normal state quasiparticles. Specifically, the conductivities are, respectively, $\sigma_x = 3.6\cdot10^{-5}\omega_p$ and $\sigma_z = 1.8\cdot10^{-7}\omega_p$.

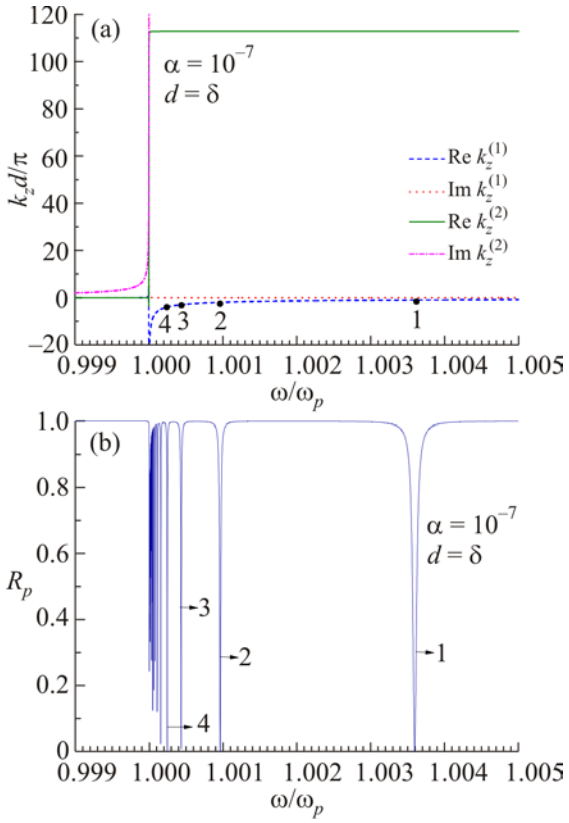

Fig. 2. (Color online) (a) Dispersion relation $k_z^{(s)}(\omega)$ for p-polarized modes in a Bi2212 superconductor at $\theta = 75^\circ$ in the quasi-local case ($\alpha = 10^{-7}$). (b) Reflectivity spectrum for a Bi2212 superconductor slab of thickness $d = \delta$ with the parameters $\sigma_x = 3.6\cdot10^{-5}\omega_p$ and $\sigma_z = 1.8\cdot10^{-7}\omega_p$.

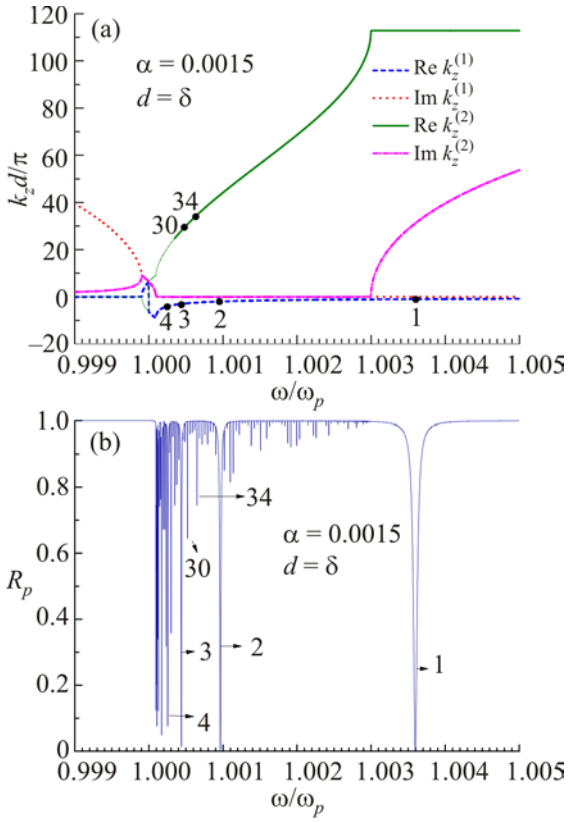

Fig. 3. (Color online) (a) Dispersion relation $k_z^{(s)}(\omega)$ for p-polarized modes in a Bi2212 superconductor at $\theta = 75^\circ$ in the case of weak nonlocality ($\alpha = 0.0015$). (b) Reflectivity spectrum for a Bi2212 superconductor slab of thickness $d = \delta$ with the parameters $\sigma_x = 3.6\cdot10^{-5}\omega_p$ and $\sigma_z = 1.8\cdot10^{-7}\omega_p$.

According to Eq. (15), for a non-zero α there are always two additional electromagnetic modes. At the specific value of the nonlocality parameter $\alpha = 10^{-7}$, the branch with negative dispersion ($k_z^{(1)}(\omega)$) practically coincides with that of the local case ($\alpha = 0$). On the other hand, the additional electromagnetic modes ($k_z^{(2)}(\omega)$) turn out to be evanescent because the imaginary part $\Im k_z^{(2)}$ is much larger than the real part $\Re k_z^{(2)}$ (see Fig. 2(a)). The black dots in the figure stand for the frequency positions where the Fabry–Perot condition is satisfied ($|\Re k_z^{(1)} d| = n\pi$, $n = 1, 2 \ldots$), and the corresponding resonances appear in the far infrared spectrum for $\alpha = 10^{-7}$ (Fig. 2(b)). This spectrum has resonances at the same frequencies as in reflectivity and transmissivity spectra for the local case with $\theta = 75^\circ$ (see Fig. 3 in Ref. 13).

3.2. Weak nonlocality

In Fig. 3, the calculations were carried out with $\alpha = 0.0015$, whereas the other parameters are the same as in Fig. 2. As is seen, the dispersion relation of the additional electromagnetic modes (the branch for $k_z^{(2)}(\omega)$) now possesses a pass band of positive dispersion just above the Josephson plasma frequency. For this reason, the reflectivity spectrum (Fig. 3(b)) exhibits Fabry–Perot resonances associated not only with the modes of negative dispersion ($k_z^{(1)}(\omega)$ branch), but also with the additional modes. The number of the later resonances is rather large because the wave number $k_z^{(2)}(\omega)$, being almost real in the pass band, rapidly increases with frequency ω until it reaches the border of the first Brillouin zone ($\Re k_z^{(2)} D/\pi = 1$ or, equivalently, $\Re k_z^{(2)} d/\pi = 112.83$). Notice that the additional Fabry–Perot resonances are weaker and narrower than the resonances associated with the electromagnetic modes with negative dispersion.

3.3. Strong nonlocality

The dispersion relation $k_z^{(s)}(\omega)$ for the case when the nonlocality parameter has a realistic value ($\alpha = 0.05$ [10,11,19]) for a Bi2212 superconductor is shown in Fig. 4(a), and the respective p-polarization reflectivity for a layered high-temperature slab with thickness $d = \delta$ is presented in Fig. 4(b). In the numerical calculations of the curves we used very small conductivities $\sigma_x = 3.6\cdot10^{-5}\omega_p$ and $\sigma_z = 1.8\cdot10^{-7}\omega_p$, producing a rather small energy dissipation in the layered high-temperature superconductor. Although the value $\alpha = 0.05$ could be considered

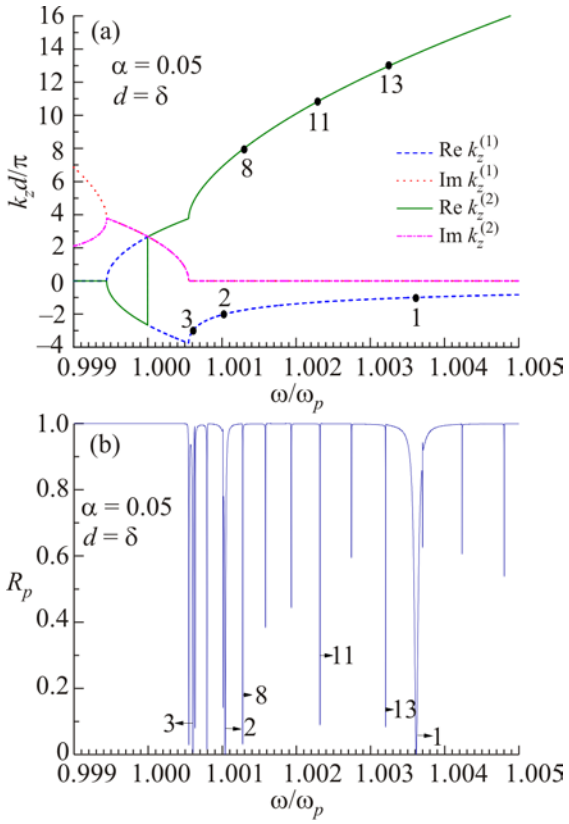

Fig. 4. (Color online) (a) Dispersion relation $k_z^{(s)}(\omega)$ for p-polarized modes in a Bi2212 superconductor at $\theta = 75^\circ$ in the case of strong nonlocality ($\alpha = 0.05$). (b) Reflectivity spectrum for a Bi2212 superconductor slab of thickness $d = \delta$ with the parameters $\sigma_x = 3.6\cdot10^{-5}\omega_p$ and $\sigma_z = 1.8\cdot10^{-7}\omega_p$.

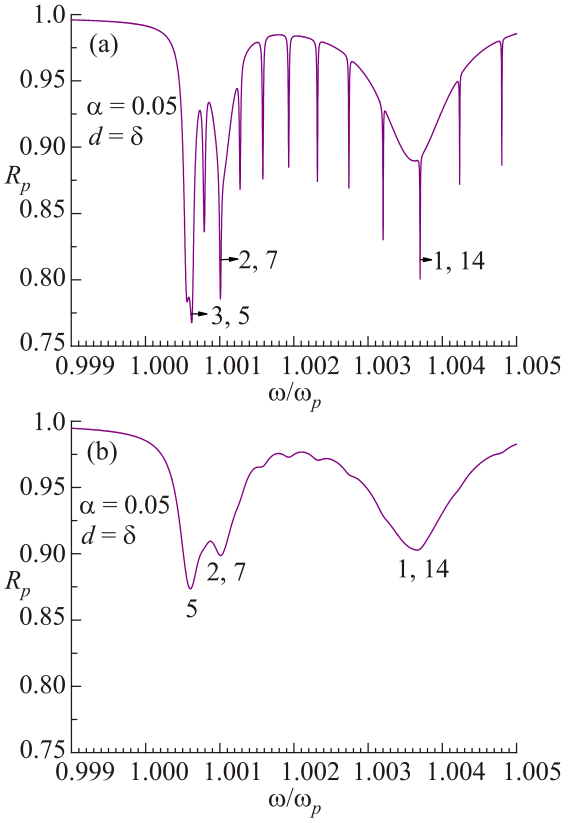

Fig. 5. (Color online) Effect of energy dissipation on the p-polarization reflectivity spectrum for a Bi2212 superconductor slab of thickness $d = \delta$ with nonlocality parameter $\alpha = 0.05$ and at $\theta = 75^\circ$ as in Fig. 4. Curve in panel (a) was calculated with $\sigma_x = 3.6\cdot10^{4}\omega_p$ and $\sigma_z = 1.8\cdot10^{-7}\omega_p$. In panel (b), $\sigma_x = 3.6\cdot10^{4}\omega_p$ and $\sigma_z = 1.8\cdot10^{-4}\omega_p$.

small, the nonlocality in this case is well developed and sufficiently strong. Indeed, with $\alpha = 0.05$, the resonances associated with the quantization of the wave vectors, corresponding to the branch of positive dispersion (additional modes), appear in a wide frequency interval and are clearly separated from each other (see Fig. 4).

In the panels of Fig. 5 we show p-polarization reflectivity spectra for a superconductor slab as that of Fig. 4, but with a typical large value of the in-plane component of the quasiparticle conductivity $\sigma_x = 3.6\cdot10^{4}\omega_p$ [11,20–22] and two different small values of the perpendicular component: $\sigma_z = 1.8\cdot10^{-7}\omega_p$ (panel (a)) and $\sigma_z = 1.8\cdot10^{-4}\omega_p$ (panel (b)). Interestingly, the large value of the conductivity component σ_x increases the light absorption in the superconductor and, consequently, the reflectivity has broad minima around the first resonances ($n = 1, 2, 3$) of the quantized modes with negative dispersion. As it is seen, the resonances associated with the quantized additional modes are practically unaffected by σ_x. The later resonances are smoothed out with increasing the perpendicular component of the conductivity, namely σ_z (compare panels (a) and (b)).

In panel (a) of Fig. 6 we show the p-polarization reflectivity spectra for Bi2212 superconductor slabs of thicknesses $d = \delta$, $d = 4\delta$ and $d = 8\delta$, which were calculated by using realistic values for both in-plane ($\sigma_x = 3.6\cdot10^{4}\omega_p$ [11,20–22]) and transverse ($\sigma_z = 1.8\cdot10^{-3}\omega_p$ [11,22,23]) conductivities. The dispersion relation for the electromagnetic modes in the layered superconductor is plotted in the subfigure 6(b). There, the black dots indicate the frequency and wave vector on the dispersion relation curve, where the Fabry–Perot condition for a superconductor slab of thickness $d = 8\delta$ is satisfied. The dots positions are in good agreement with the observed resonances in the corresponding reflectivity spectrum shown in the panel (a). Notice that only the resonances of electromagnetic modes with negative dispersion are well-resolved. For this reason, the dips of the resonances in the reflectivity spectra are shifted towards higher frequencies when the thickness slab is increased (compare the curves in Fig. 6(a)).

Figure 7(a) exhibits the p-polarization reflectivity spectra for superconductor slabs of thicknesses smaller than the skin depth δ: $d = 0.10\delta$, $d = 0.15\delta$ and $d = 0.25\delta$. The panel (b) of Fig. 7 shows the dispersion relation curve with the positions of the frequencies where the Fabry–Perot condition is satisfied in a slab of thickness $d = 0.10\delta$. Because of the small slab thickness, only the wave vectors of

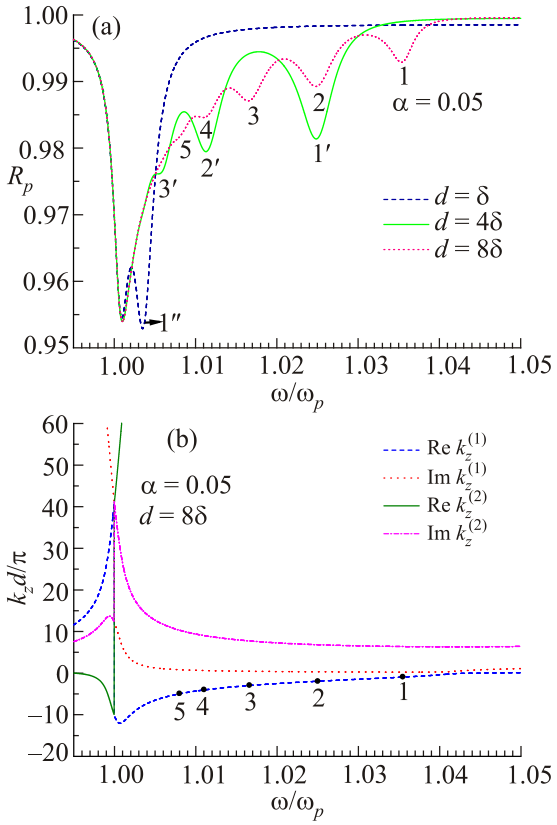

Fig. 6. (Color online) (a) p-polarization reflectivity spectra for Bi2212 superconductor slabs of thickness $d = 1$, 4, 8δ at $\theta = 75^\circ$. The quasiparticle conductivities used are: $\sigma_x = 3.6\cdot10^4\omega_p$ and $\sigma_z = 1.8\cdot10^{-3}\omega_p$. (b) Dispersion relation $k_z^{(s)}(\omega)$ for p-polarized modes in a Bi2212 superconductor.

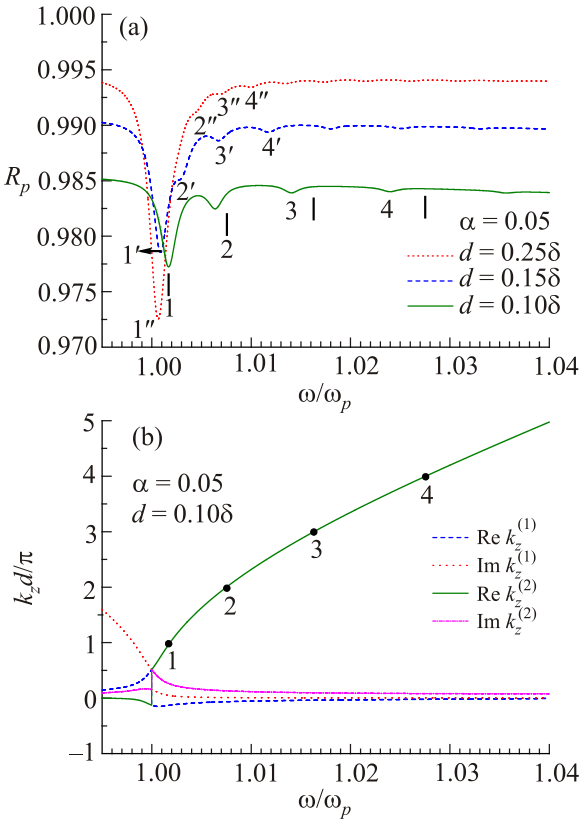

Fig. 7. (Color online) (a) p-polarization reflectivity spectra for Bi2212 superconductor slabs of thickness $d = 0.1$, 0.15, 0.25δ at $\theta = 75^\circ$. The quasiparticle conductivities used are: $\sigma_x = 3.6\cdot10^4\omega_p$ and $\sigma_z = 1.8\cdot10^{-3}\omega_p$. (b) Dispersion relation $k_z^{(s)}(\omega)$ for p-polarized modes in a Bi2212 superconductor.

the additional electromagnetic modes are quantized, leading to the appearance of discernible resonances in the p-polarization reflectivity spectrum (see panel (a)). As is also seen, the dips of the resonances in the reflectivity spectrum are shifted towards higher frequencies when the slab thickness is decreased. There is another remarkable feature of the reflectivity spectra for thin slabs: the position of the reflectivity resonances turn out to be slightly shifted to lower frequencies with respect to the frequencies where the Fabry–Perot condition is satisfied. In fact, in Fig. 7(a) the small lines next to the numbers, labeling the resonances, indicate the frequencies where the Fabry–Perot condition is really satisfied. This shift of the resonances is attributed to the type of the additional boundary conditions, (31) and (32), used in our calculations since the optical spectra of nonlocal media depend on the ABCs.

4. Discussion of the results

Because of the nonlocality of the optical response of a layered high-temperature superconductor slab, i.e., as a result of the wave vector dependence of its average permittivity tensor $\overleftrightarrow{\varepsilon}_{av}(k_z^{(s)})$ (Eqs. (7)–(9)), for a given frequency four p-polarized electromagnetic modes can propagate through the sample. For this reason, to calculate their amplitudes it was necessary to apply the Maxwell boundary conditions (22) together with the ABCs derived in subsection 2.3, namely Eqs. (31) and (32). Using the classification of ABCs, which is employed for other nonlocal media such as excitonic ones, the above derived ABCs correspond to the generalized ABCs [24]:

$$\alpha_{z,0}P_z^{(s)}(0) + \beta_{z,0}\partial P_z^{(s)}(0)/\partial z = 0,$$

$$\alpha_{z,d}P_z^{(s)}(d) + \beta_{z,d}\partial P_z^{(s)}(d)/\partial z = 0, \qquad (33)$$

with $\alpha_{z,0} = \alpha_{z,d} = 1$ and $\beta_{z,0} = -\beta_{z,d} = -D/2$. In our case, the applied here ABCs came from the absence of Josephson junctions just outside the superconductor sample. The choice of the ABCs can qualitatively change the optical properties of nonlocal systems, e.g., the reflectivity and transmissivity, since these nonlocal spectra are sensitive to the microstructure of the sample surfaces. Therefore, to properly describe the nonlocal response of a superconductor, the parameters $\alpha_{z,0}$, $\alpha_{z,d}$, $\beta_{z,0}$, and $\beta_{z,d}$ in the generalized ABCs (33) can be fitted to experimental optical spectra.

Our results presented in previous section demonstrate that, even for realistic large in-plane (σ_x) and transverse (σ_z) components of quasiparticle conductivity, the *p*-polarization reflectivity spectra for Bi2212 superconductor slabs with thickness d larger than the skin depth $\delta = \lambda_{||} = c/(\gamma\omega_p\sqrt{\varepsilon})$ ($d > \delta$) have well-resolved resonances associated with the quantization of the wave vector for electromagnetic modes with negative dispersion. In contrast, when the thickness d is smaller than δ ($d < \delta$) the optical spectra exhibit separated resonances originated by Fabry–Perot resonances of the additional (short-wave length) electromagnetic modes inside the superconductor slab.

In Ref. 13, where a local average permittivity tensor was considered, it was demonstrated that the quantized electromagnetic modes in a layered superconductor slab are quasi-longitudinal because of the large anisotropy of its dielectric response, i.e., a strong contrast between the permittivity components ($|\varepsilon_x| \gg |\varepsilon_z|$). Indeed, as follows from Eq. (13), we obtain

$$\frac{|k_z^{(s)}|}{k_x} \approx \sqrt{\frac{-\varepsilon_x}{\varepsilon_z}} \gg 1, \tag{34}$$

and from the Maxwell equation $\nabla \cdot \mathbf{D} = 0$, we get

$$|E_z| = \left|\frac{-k_x\varepsilon_x}{k_z^{(s)}\varepsilon_z}E_x\right| \approx \left|\frac{k_z^{(s)}}{k_x}E_x\right| \gg |E_x|. \tag{35}$$

Hence, the z component of the electric field is much larger than its x component. This conclusion is also valid for the additional short-wavelength electromagnetic modes generated in the nonlocal case because they have even larger wave numbers $k_z^{(s)}$ ($|k_z^{(s)}| \gg k_x$) and the inequality (35) is fulfilled.

5. Conclusions

As a result of the spatially-dispersive (nonlocal) optical response of layered high-temperature superconductors, additional electromagnetic modes are generated in the *p*-polarization geometry. The calculated *p*-polarization THz spectra for a Bi2212 superconductor slab show very narrow resonances associated with the quantization of the wave vectors of long-wavelength electromagnetic modes, having negative dispersion, and short-wavelength additional modes of positive dispersion, in the frequency interval just above the characteristic Josephson plasma frequency of the superconductor. The frequency positions of the resonances are determined by the nonlocality parameter, the slab thickness and the angle of incidence. In the case when the thickness slab is larger than the skin depth ($d > \delta$), the discernible resonances in reflectivity spectra are due to the excitation of electromagnetic modes with anomalous dispersion and, therefore, they undergo a shift towards higher frequencies as the slab thickness is increased. At slab thicknesses smaller than the skin depth ($d < \delta$), the dips of the resonances are mainly associated with quantized additional electromagnetic modes. Because of their positive dispersion, such resonances are shifted towards higher frequencies as the slab thickness is decreased. We have found that the quantized electromagnetic modes are quasi-longitudinal because of the strong anisotropy in the nonlocal optical response of the high-temperature superconductor.

Acknowledgments

This work was partially supported by CONACYT (grant CB-2012-01-183673) and VIEP-BUAP (grant 100160855-VIEP2018).

1. Takanari Kashiwagi, Manabu Tsujimoto, Takashi Yamamoto, Hidetoshi Minami, Kazuhiro Yamaki, Kaveh Delfanazari, Kota Deguchi, Naoki Orita, Takashi Koike, Ryo Nakayama, Takeo Kitamura, Masashi Sawamura, Shota Hagino, Kazuya Ishida, Krsto Ivanovic, Hidehiro Asai, Masashi Tachiki, R.A. Klemm, and Kazuo Kadowaki, *Jpn. J. Appl. Phys.* **51**, 010113 (2012).
2. Kaveh Delfanazari, Hidehiro Asai, Manabu Tsujimoto, Takanari Kashiwagi, Takeo Kitamura, Kazuya Ishida, Chiharu Watanabe, Shunsuke Sekimoto, Takashi Yamamoto, Hidetoshi Minami, Masashi Tachiki, Richard A. Klemm, Toshiaki Hattori, and Kazuo Kadowaki, *J. Infrared Milli Terahz Waves* **35**, 131 (2014).
3. T Kashiwagi, H Kubo, K Sakamoto, T Yuasa, Y Tanabe, C Watanabe, T Tanaka, Y Komori, R Ota, G Kuwano, K Nakamura, T Katsuragawa, M Tsujimoto, T Yamamoto, R Yoshizaki, H Minami, K Kadowaki, and RA Klemm, *Supercond. Sci. Technol.* **30**, 074008 (2017).
4. S. Sakai, P. Bodin, and N.F. Pedersen, *J. Appl. Phys.* **73**, 2411 (1993).
5. T. Koyama and M. Tachiki, *Phys. Rev. B* **54**, 16183 (1996).
6. A.E. Koshelev and I. Aranson, *Phys. Rev. B* **64**, 174508 (2001).
7. T. Koyama, *Physica C* **367**, 355 (2002).
8. S. Savel'ev, V.A. Yampol'skii, A.L. Rakhmanov, and F. Nori, *Rep. Prog. Phys.* **73**, 026501 (2010).
9. Y. Laplace and A. Cavalleri, *Advance Phys. X* **1**, 387 (2016).
10. Ch. Helm and L.N. Bulaevskii, *Phys. Rev. B* **66**, 094514 (2002).
11. A.L. Rakhmanov, V.A. Yampol'skii, J.A. Fan, F. Capasso, and F. Nori, *Phys. Rev. B* **81**, 075101 (2010).
12. T.M. Slipchenko, D.V. Kadygrob, D. Bogdanis, V.A. Yampol'skii, and A. A. Krokhin, *Phys. Rev. B* **84**, 224512 (2011).
13. S. Cortés-López and F. Pérez-Rodríguez, *Acta Phys. Pol. A* **130**, 641 (2016).
14. S.S. Apostolov, V.I. Havrilenko, Z.A. Maizelis, and V.A. Yampol'skii, *Fiz. Nizk. Temp.* **43**, 360 (2017) [*Low Temp. Phys.* **43**, 296 (2017)].
15. S.S. Apostolov, N.M. Makarov, and V.A. Yampol'skii, *Fiz. Nizk. Temp.* **43**, 1059 (2017) [*Low Temp. Phys.* **43**, 848 (2017)].
16. S.S. Apostolov, N.M. Makarov, and V.A. Yampol'skii, *Phys. Rev. B* **97**, 024510 (2018).

17. D.V. Kadygrob, N.M. Makarov, F. Pérez-Rodríguez, T.M. Slipchenko, and V.A. Yampol'skii, *New J. Phys.* **15**, 023040 (2013).
18. D.V. Kadygrob and V.A. Yampol'skii, *Fiz. Nizk. Temp.* **40**, 910 (2014) [*Low Temp. Phys.* **40**, 707 (2014)].
19. S. Rother, Y. Koval, P. Müller, R. Kleiner, D.A. Ryndyk, J. Keller, and C. Helm, *Phys. Rev. B* **67**, 024510 (2003).
20. S.-F. Lee, D.C. Morgan, R.J. Ormeno, D.M. Broun, R.A. Doyle, J.R. Waldram, and K. Kadowaki, *Phys. Rev. Lett.* **77**, 735 (1996).
21. H. Kitano T. Hanaguri, Y. Tsuchiya, K. Iwaya, R. Abiru, and A. Maeda, *J. Low Temp. Phys.* **117**, 1241 (1999).
22. Yu.I. Latyshev, A.E. Koshelev, and L.N. Bulaevskii, *Phys. Rev. B* **68**, 134504 (2003).
23. Yu.I. Latyshev, T. Yamashita, L.N. Bulaevskii, M.J. Graf, A.V. Balatsky, and M.P. Maley, *Phys. Rev. Lett.* **82**, 5345 (1999).
24. E.A. Kaner, A.A. Krokhin, and N.M. Makarov, *Spatial Dispersion and Surface Electromagnetic Absorption in Metals*, in the book *Spatial Dispersion in Solids and Plasmas*, P. Halevi (ed.), Elsevier, Amsterdam, vol. 1, Chap. 6, 339 (1992).

Нелокальний оптичний відгук шаруватої високотемпературної надпровідної пластини

S. Cortés-López, F. Pérez-Rodríguez

Теоретично вивчено вплив просторової дисперсії на оптичний відгук шаруватої високотемпературної надпровідної пластини. Нелокальність анізотропного шаруватого надпровідника обумовлена залежністю від хвильового вектора середньої величини тензора діелектричної проникності та призводить до генерації додаткових електромагнітних мод, частота яких перевищує характерну джозефсонівську плазмову частоту, що відповідає терагерцовому діапазону. Обчислено *p*-поляризаційні оптичні спектри в надпровідній пластині $Bi_2Sr_2CaCu_2O_{8+\delta}$ (Bi2212), які вказують на наявність дуже вузьких резонансів, пов'язаних з квантуванням хвильових векторів як довгохвильових електромагнітних мод, що мають від'ємну дисперсію, так і короткохвильових додаткових (нелокальних) мод з позитивною дисперсією. Вивчено частотну залежність та залежність форми резонансів від параметра нелокальності, товщини пластини, крім того, проаналізовано поведінку різних складових в провідності квазічастинок. Встановлено, що квантовані довгохвильові моди з від'ємною дисперсією, які можуть спостерігатися в пластинах відносно великої товщини, породжують виражені резонанси в *p*-поляризаційному спектрі відбитих хвиль. З іншого боку, резонанси, пов'язані з додатковими квантовими електромагнітними модами, слабко виражені, але можуть бути чітко визначені в разі, коли товщина надпровідної пластини не перевищує найменшу магнітну довжину проникнення.

Ключові слова: шаруваті надпровідники, купратні надпровідники, метаматеріали, просторова дисперсія, тонкі лінії.

Нелокальный оптический отклик слоистой высокотемпературной сверхпроводящей пластины

S. Cortés-López, F. Pérez-Rodríguez

Теоретически изучено влияние пространственной дисперсии на оптический отклик слоистой высокотемпературной сверхпроводящей пластины. Нелокальность анизотропного слоистого сверхпроводника обусловлена зависимостью от волнового вектора средней величины тензора диэлектрической проницаемости и приводит к генерации дополнительных электромагнитных мод, частота которых превышает характерную джозефсоновскую плазменную частоту, что соответствует терагерцовому диапазону. Вычислены *p*-поляризационные оптические спектры в сверхпроводящей пластине $Bi_2Sr_2CaCu_2O_{8+\delta}$ (Bi2212), которые указывают на наличие очень узких резонансов, связанных с квантованием волновых векторов как длинноволновых электромагнитных мод, имеющих отрицательную дисперсию, так и коротковолновых дополнительных (нелокальных) мод с положительной дисперсией. Изучена частотная зависимость и зависимость формы резонансов от параметра нелокальности, толщины пластины, кроме того, проанализировано поведение различных составляющих в проводимости квазичастиц. Установлено, что квантованные длинноволновые моды с отрицательной дисперсией, которые могут наблюдаться в пластинах относительно большой толщины, порождают выраженные резонансы в *p*-поляризационном спектре отраженных волн. С другой стороны, резонансы, связанные с дополнительными квантованными электромагнитными модами, слабо выражены, но могут быть четко определены в случае, когда толщина сверхпроводящей пластины не превышает наименьшую магнитную длину проникновения.

Ключевые слова: слоистые сверхпроводники, купратные сверхпроводники, метаматериалы, пространственная дисперсия, тонкие линии.